Charge-density correlations in pressurized liquid lithium calculated using *ab initio* molecular dynamics

Taras Bryk,[1,2] Ivan Klevets,[1] Giancarlo Ruocco,[3,4] Tullio Scopigno,[3,5] and Ari P. Seitsonen[6,*]

[1]*Institute for Condensed Matter Physics of the National Academy of Sciences of Ukraine, 1 Svientsitskii Street, UA-79011 Lviv, Ukraine*

[2]*Institute of Applied Mathematics and Fundamental Sciences, Lviv Polytechnic National University, 79013 Lviv, Ukraine*

[3]*Dipartimento di Fisica, Universita di Roma La Sapienza, I-00185 Roma, Italy*

[4]*Center for Life Nano Science @Sapienza, Istituto Italiano di Tecnologia, 295 Viale Regina Elena, I-00161 Roma, Italy*

[5]*IPCF-CNR, Universita di Roma, I-00185 Roma, Italy*

[6]*Institut für Chemie, University of Zürich, CH-8057 Zürich, Switzerland*

(Received 20 February 2014; revised manuscript received 17 June 2014; published 15 July 2014)

Static and dynamic autocorrelations of charge density, composed of positive point ions and instantaneous distribution of electron density, are studied in liquid Li in a pressure range from ambient to 186 GPa using *ab initio* molecular dynamics simulations. It is shown analytically that the long-wavelength limit of the charge-charge static structure factor $S_{QQ}(k)$ of liquid metals is proportional to k^4. Time-dependent charge-charge correlations in liquid Li at low pressures show identical relaxation as the density-density time correlation functions, in complete agreement with the linear response theory, whereas at extreme pressures we observed different relaxation of the charge and density autocorrelations. The static and dynamic properties of a part of electron density, that corresponds to the nonspherical distribution around ions, are discussed.

DOI: 10.1103/PhysRevB.90.014202 PACS number(s): 61.20.Ja, 61.20.Lc, 61.25.Mv, 62.50.−p

I. INTRODUCTION

Simple alkali metals Li, Na, K, Rb, Cs reveal fascinating changes of structural, electronic, and dynamic properties under pressures. Numerous structural transformations were found in the solid alkali metals with increasing pressure [1], while the physical properties of liquid alkalis under high pressure were essentially not studied. There were reports on rapid changes in molten Na under high pressure [2]. A tetrahedral clustering in liquid Li that takes place at pressure ∼150 GPa and leads to the tetrahedral order of the closest of the nearest neighbors of each ion was reported in [3]. The electron wave functions of the highly compressed Li were found [3] to become mostly of p type and localized in the interstitial regions. Recently *ab initio* simulations of liquid Rb [4], performed in a pressure range up to 27.4 GPa at $T = 573$ K, revealed a dynamic crossover observed in the behavior of self-diffusion and sound propagation as functions of increasing density. Detailed analysis of electronic and static properties revealed that the observed dynamic crossover is a consequence of a structural transition at pressure ∼12.9 GPa to a low-coordinated phase of liquid Rb with partial localization of electrons.

Liquid alkali metals at ambient conditions can be successfully explored by computer simulations with solely effective pair potentials [5,6]. However this is not the case when the liquid metals are studied under high pressure. Essentially non-free-electron distribution of electron density in solid and liquid metals under high pressure [7,8] is caused by squeezing out the electron density into interstitial regions (pockets). In the case of crystals (such as Li [3,7] or Na [2]) at high pressures those pockets can become isolated, separated by ionic cores, and the system turns into a nonmetal. In liquid alkalis at high pressures, due to diffusivity of ions the connectivity of pockets always remains nonvanishing and the system is metallic (or semimetallic) up to the highest studied pressures [2–4].

However there have been no attempts to characterize the electron and in general charge distributions in liquid metals at high pressures. It is not clear how the essentially non-free-electron density distribution will affect the charge correlations, which at ambient conditions can be well described by the linear response theory (LRT) [9,10]. The LRT states that the screening electron density can be represented as follows:

$$\rho_{\rm el}^{\rm scr}(k) = \chi_{\rm el}(k)\frac{4\pi Z_{\rm ion}}{k^2}\rho_{\rm ion}(k), \tag{1}$$

where $\chi_{\rm el}(k)$ is the static electron response function, $Z_{\rm ion}$ is the ionic charge, and $\rho_{\rm ion}(k)$ is the spatial Fourier component of the ionic density with wave number k. Here the screening electron density is assumed to follow the motion of the ions, and this effect is used in the derivation of effective pair potentials and classical MD simulations with electron density hidden in the Friedel-like tail of the effective potentials of metallic systems.

The effect of electron-ion correlations can be studied explicitly in the scattering experiments. In a recent study of warm dense Li [11] an analysis of experimental x-ray scattering intensities in the eV range was performed by means of electron-ion and electron-electron dynamic structure factors $S_{ei}(k,\omega)$ and $S_{ee}(k,\omega)$. Corresponding static electron-ion $S_{ei}(k)$ and electron-electron $S_{ee}(k)$ have been studied in metallic systems since the 1970s [12,13], initially using the electron density represented within the pseudopotential theory [14–17] and later taking it from *ab initio* simulations [18,19]. Very important is that for electron-ion and electron-electron static structure factors there exist exact sum rules in the long-wavelength limit:

$$\begin{aligned} S_{ei}(k\to 0) &= \sqrt{Z_{\rm ion}}S_{ii}(k\to 0),\\ S_{ee}(k\to 0) &= Z_{\rm ion}S_{ii}(k\to 0), \end{aligned} \tag{2}$$

*Present address: École Normale Supérieure, Département de Chimie, 24 rue Lhomond, F-75005 Paris, France.

where $S_{ii}(k)$ is the regular ion-ion structure factor. In binary systems such as molten salts or liquid metallic alloys the partial electron-ion structure factors have more complicated sum rules [12], that were successfully tested recently in *ab initio* simulations by comparing simulation results with analytical long-wavelength asymptotes [20,21].

More general *ab initio* studies of total charge density correlation and in particular charge-charge static structure factors $S_{QQ}(k)$, where the total charge density is composed of positive point ions and instantaneous distribution of electron density, were reported in [22,23] for the case of network-forming liquids. However, to date there have been no studies on the long-wavelength behavior of $S_{QQ}(k)$, that can be very important for explanation of behavior of metallic systems under extreme pressures. If the metallic systems could behave under extreme pressures like an ionic compound as was reported for potassium [24], this would be immediately reflected in the asymptotic long-wavelength behavior of $S_{QQ}(k)$. Moreover, it is not known how the effects of partial localization of electrons at high pressures affect the static and time-dependent charge-charge correlations in liquid metals under high pressures.

Therefore the main aim of this study was in calculations of the total charge static and time-dependent correlations from *ab initio* MD simulations in the case of liquid Li in a wide range of pressures and the analysis of them in order to understand the long-wavelength asymptotes of $S_{QQ}(k)$ and possible effects of high pressures on these correlations. The remaining paper is organized as follows: In the next section we give details of our *ab initio* simulations. The third sections contains analytical study of the long-wavelength asymptotes of static charge-charge correlations. We will compare *ab initio* results with analytical asymptotes and will consider the effect of pressure on time-dependent total charge correlations. The last section will contain conclusions of this study.

II. *AB INITIO* MOLECULAR DYNAMICS SIMULATIONS

The *ab initio* simulations were performed for liquid Li at $T = 1000$ K at seven different pressures in a range from ambient pressure up to 186 GPa using systems of 300 particles (pressures up to 68 GPa) and 600 particles (higher pressures) in the *NVT* ensemble in a cubic box with periodic boundary conditions. The time step in simulations was 1 fs, and after an equilibration over 3-4 ps depending on the system, the production runs were executed for 12 ps (12 000 time steps).

The electron-ion interactions were represented by the lithium all-electron projector augmented wave (PAW) potentials [25,26]. The plane-wave cutoff energy ($\hbar^2 K_{\max}^2/2m_e$) was 271.6 eV and the cutoff energy for the augmentation charge (in PAW methodology) was 428.4 eV. For each pressure the grid mesh for electron density was chosen to be large enough to represent the Fourier components of electron density from $-2K_{\max}$ to $2K_{\max}$. The generalized gradient approximation in the Perdew-Burke-Ernzerhof version (PBE) [27] was applied in order to account for exchange-correlation effects in the strongly nonuniform (all-electron) density of molten Li. The electron density was constructed using the single Γ point in the Brillouin zone, that is justified by quite large box size.

Up to sixty wave numbers k were sampled in the calculation of the static and time correlation functions. The smallest wave numbers in our simulations changed from $k_{\min} = 0.353$ Å^{-1} in l-Li at ambient pressure to $k_{\min} = 0.442$ Å^{-1} at 186 GPa. The calculated static and time correlation functions were averaged over all possible directions of wave vectors with the same absolute value.

III. ANALYTIC LONG-WAVELENGTH ASYMPTOTE OF STATIC CHARGE-CHARGE CORRELATIONS IN LIQUID METALS

We define the total charge density in a liquid metal according to Ref. [9] as

$$Q(k,t) = \frac{1}{\sqrt{N}}\left[Z_{\text{ion}}\sum_i^N e^{-i\mathbf{k}\mathbf{R}_i(t)} - \rho_{\text{el}}(k,t)\right], \quad (3)$$

where N is the number of particles in the MD box, Z_{ion} is the bare charge of ionic pseudopotential, and $\rho_{\text{el}}(k)$ the Fourier components of electron density corresponding to instantaneous ionic positions $\{\mathbf{R}_i\}$. Making use of the analytical expression for electron density from linear response theory in Eq. (1) one obtains

$$\begin{aligned} Q^{LRT}(k,t) &= \frac{1}{\sqrt{N}}\left[Z_{\text{ion}}\sum_i^N e^{-i\mathbf{k}\mathbf{R}_i(t)} - \rho_{\text{el}}^{\text{scr}}(k,t)\right] \\ &= \frac{1}{\sqrt{N}} Z_{\text{ion}}\left[1 - \chi_{\text{el}}(k)\frac{4\pi Z_{\text{ion}}}{k^2}\right]\sum_i^N e^{-i\mathbf{k}\mathbf{R}_i(t)}. \quad (4) \end{aligned}$$

In the long-wavelength limit and random phase approximation (RPA) for the electron density response function [9] this expression reduces to

$$Q^{LRT}(k\to 0,t) = Z_{\text{ion}}\left[\frac{k^2}{k_{\text{TF}}^2} - G(k/k_{\text{F}})\right]\rho_{\text{ion}}(k,t), \quad (5)$$

where k_{TF} is the Thomas-Fermi wave number, k_{F} the Fermi wave number, and $G(k/k_{\text{F}})$ is the local field correction, which in the long-wavelength limit is proportional to k^2 (Ref. [28]). Hence, it follows immediately that within the linear response theory the total charge static structure factor in liquid metals,

$$S_{QQ}(k) = \langle Q(k)Q(-k)\rangle, \quad (6)$$

takes in the long-wavelength limit the form

$$\lim_{k\to 0} S_{QQ}(k) = Z_{\text{ion}}^2\left[\frac{k^2}{k_{\text{TF}}^2} - G(k/k_{\text{F}})\right]^2 S_{ii}(k\to 0). \quad (7)$$

Since the long-wavelength limit of the ionic structure factor $S_{ii}(k\to 0) = k_B T\rho\kappa_T$ tends to a nonzero constant (if the system is not in the vicinity of a phase transition), defined by the temperature T, the mass-density of the system ρ and the isothermal compressibility κ_T, one may conclude that the total charge structure factor $S_{QQ}(k)$ of liquid metals should be a function of k^4 in the long-wavelength limit:

$$\lim_{k\to 0} S_{QQ}(k) = \alpha k^4. \quad (8)$$

In the short-wavelength limit one may take into account expression (3) and the fact that the Fourier components of the electron density decay to zero in the limit $k\to\infty$, leading

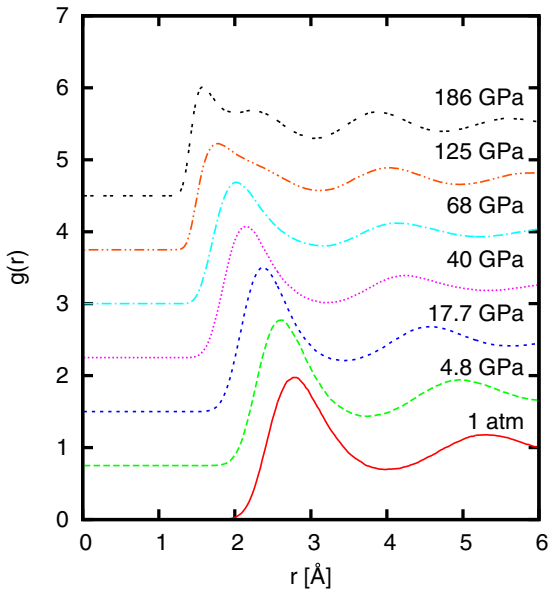

FIG. 1. (Color online) Pair distribution function in liquid Li at 1000 K at seven different pressures. A progressive vertical shift of 0.75 was applied for the sequence of pair distribution functions.

to the asymptote

$$\lim_{k\to\infty} S_{QQ}(k) = Z_{\rm ion}^2 S_{ii}(k\to\infty) = Z_{\rm ion}^2. \qquad (9)$$

In the actual case of liquid Li with the all-electron PAW potential used in the *ab initio* molecular dynamics, the ionic charge was $Z = 3$ and therefore in the short-wavelength limit the charge-charge static structure factors $S_{QQ}(k)$ tend to the value $Z_{\rm ion}^2 = 9$.

Since the screening of ionic charge in metallic systems differs from the one in nonmetallic systems with long-range Coulomb interactions, such as ionic crystals or molten salts, the long-wavelength asymptote (8) of $S_{QQ}(k)$ in liquid metals is different from the $S_{QQ}^{\rm ionic}(k\to 0)$, for which [29]

$$\lim_{k\to 0} S_{QQ}^{\rm ionic}(k) \sim k^2. \qquad (10)$$

This sensitivity of the long-wavelength asymptote of the charge-charge structure factor to the ionic or metallic state of the system can be very important for identifying the metallic/ionic phase in the above-mentioned case of potassium at extreme pressures [24] or in metallization of hydrogen at high pressures via an intermediate phase with partially molecular and partially ionized hydrogens [30].

IV. STATIC CORRELATIONS CALCULATED FROM *AB INITIO* MD SIMULATIONS

The pair distribution functions in liquid Li at $T = 1000$ K at the different pressures are shown in Fig. 1. The general tendency of the applied pressure is the shift in the first maximum of the pair distribution function from 2.78 Å at ambient pressure to 1.59 Å at $P = 186$ GPa with the corresponding reduction of its amplitude $g(r_{\rm max})$ from 1.98 to 1.51. As expected, due to increase of pressure the first coordination shell gets smaller. At pressures above 100 GPa we observed a gradual increase of a shoulder in the region $r \sim 2.2$ Å followed by a splitting of the first peak in the pair distribution function into two separated maxima at the highest studied pressure, 186 GPa. The number of the nearest neighbors, calculated from the $g(r)$ at 186 GPa at the distance 1.8 Å, is close to 4. The angular distribution for the closest of the nearest neighbors in the sphere $R_{\rm cut} = 1.6$ Å shows almost perfect distribution around the angle of 109° (left panel in Fig. 2). This is an effect reported in Ref. [3] as tetrahedral clustering in liquid Li at pressures above 150 GPa. The orbital-moment projected density of electronic states (right panel in Fig. 2) shows the strong p character of states at the Fermi level predicted in Ref. [3], which explains the appearance of the tetrahedral structures of the closest of the nearest neighbors in liquid Li at high pressures. Our results at $P = 186$ GPa, obtained from simulations with 600 particles, completely support the previous findings observed with a much smaller number of particles [3].

The static ion-ion structure factors, obtained as the statistical average $S_{ii}(k) = \langle \rho_{\rm ion}(k)\rho_{\rm ion}(-k)\rangle$ of density-density correlations at the seven pressures (see Fig. 3), show the general tendency of shifting the first diffraction peak (FDP) towards higher wave numbers: from 2.57 Å^{-1} at ambient pressure to 3.54 Å^{-1} at 186 GPa. In the pressure range 40–125 GPa we observed a shoulder on the right slope of the FDP which shifted from $k \sim 3.5$ Å^{-1} to higher wave numbers

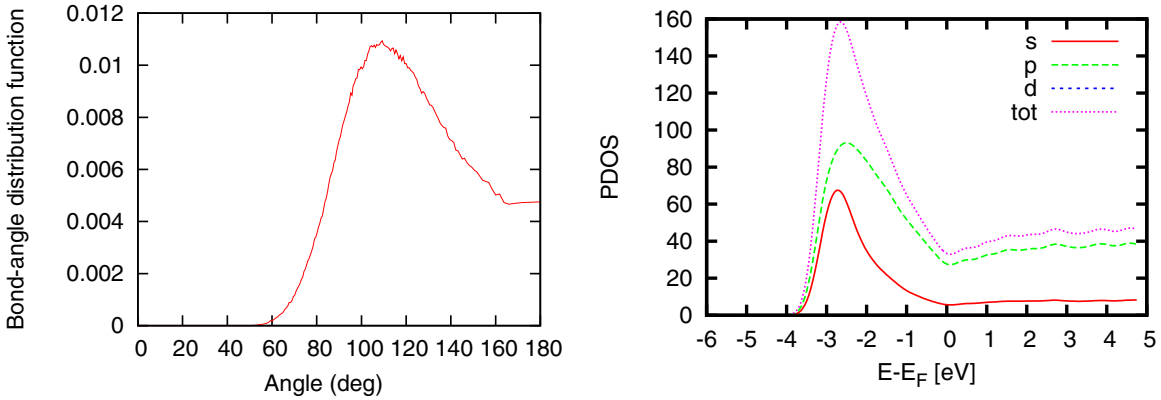

FIG. 2. (Color online) Left: Bond-angle distribution between the closest of the nearest neighbor atoms in the sphere $R_{\rm cut} = 1.6$ Å in liquid Li at $T = 1000$ K and $P = 186$ GPa. Right: l-projected density of electronic states.

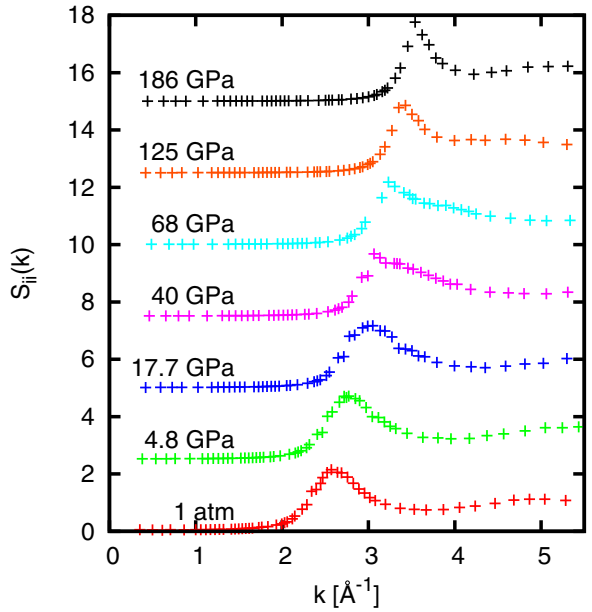

FIG. 3. (Color online) Ion-ion static structure factors $S_{ii}(k)$ in liquid Li at 1000 K at seven different pressures. A progressive vertical shift of 2.50 was applied for the sequence of the static structure factors.

$\sim$4.5 Å^{-1} at 125 GPa. This shoulder is connected to the progressive broadening of the first coordination shell above 40 GPa (see Fig. 1) until the split of the first coordination shell into two well-separated maxima in the pair distribution function observed at 186 GPa mentioned above.

In order to calculate the total charge correlations we had to check the electron-ion structure factors and their consistency with the analytical sum rules (2). The calculated electron-ion structure factors $S_{ei}(k)$ looked very similar to the $S_{ii}(k)$. Therefore in Fig. 4 we show the ratio $S_{ei}(k)/S_{ii}(k)$. Since we used in simulations the all-electron potential for Li, the total electron density is composed of three electrons per atom, and thus in the long-wavelength limit the ratio $S_{ei}(k)/S_{ii}(k)$, according to (2), must tend to $\sqrt{3}$. This is clearly seen in Fig. 4 at the four different pressures shown.

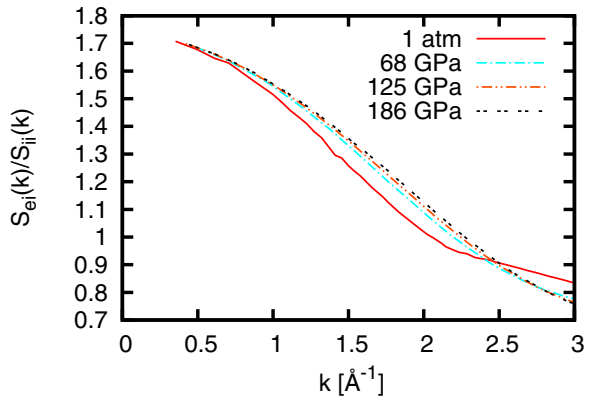

FIG. 4. (Color online) Ratio of the electron-ion $S_{ei}(k)$ to ion-ion static structure factor $S_{ii}(k)$ at different pressures. In the long-wavelength limit this ratio is in perfect agreement with the sum rule (2).

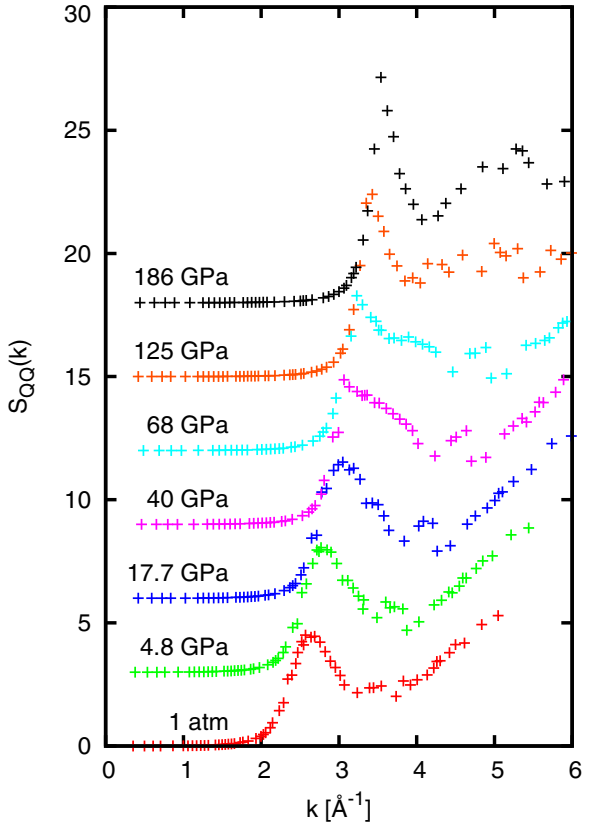

FIG. 5. (Color online) Charge-charge static structure factor $S_{QQ}(k)$ at the seven different pressures in liquid Li at 1000 K. A progressive vertical shift of 3.00 was applied for the sequence of the static structure factors.

The total charge structure factor $S_{QQ}(k)$ at different pressures is shown in Fig. 5. Three main features of $S_{QQ}(k)$ are observed in its pressure dependence: the $S_{QQ}(k)$ curves tend to zero in the long-wavelength limit due to the electroneutrality condition; at the location of FDP in $S_{ii}(k)$ they show a pronounced peak, whose amplitude increases with pressure from 4.5 at 1 atmosphere to 9.2 at $P = 186$ GPa; there appears with pressure a second maximum of $S_{QQ}(k)$, increasing in amplitude from 2.7 at 1 atmosphere to 6.45 at $P = 186$ GPa and shifting its location from $k \sim 3.5$ Å^{-1} to ~ 5.3 Å^{-1} correspondingly; in the short-wavelength limit they tend to the value Z^2_{ion}. One of the most interesting issues is the long-wavelength limit of $S_{QQ}(k)$. In Sec. III we predicted on the basis of the linear response theory that the analytical long-wavelength asymptote $\sim k^4$, Eqs. (7), (8). The double-logarithmic plot of the long-wavelength behavior shows that the simulations at all pressures are in perfect agreement with the predicted $\sim k^4$ asymptote of $S_{QQ}(k \to 0)$ (see Fig. 6). This means that up to the pressure of 186 GPa liquid Li at 1000 K remains metallic, which is in agreement with the electronic density of states in Fig. 2 at the highest pressure. The density dependence of the coefficient α in the long-wavelength asymptote (8) is shown in Fig. 7. In the limit of high densities (small r_s) the quadratic dependence $\sim r_s^2$ predicted within the RPA (Ref. [28]) is recovered, which is another check of the consistency of our *ab initio* study of the charge-charge correlations in high-pressure Li.

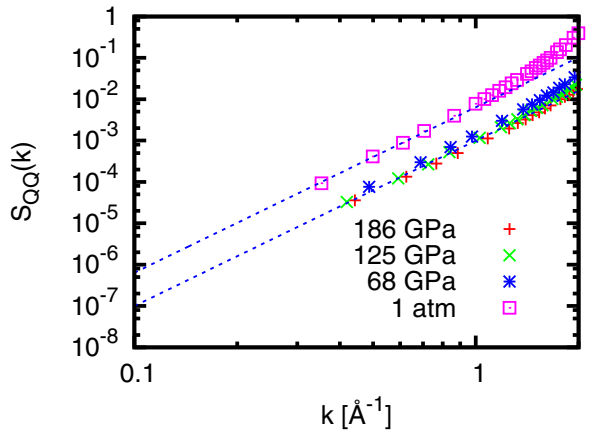

FIG. 6. (Color online) Long-wavelength asymptotes of the charge-charge static structure factors $S_{QQ}(k)$ at four pressures on double-logarithmic scale. The straight lines show the $\sim k^4$ dependence.

The higher the pressure is, the more the electron density distribution is nonspherical between the ions. In Fig. 8 we show the isosurface of the electron localization function (ELF) [31] with the ELF value 0.85 in three snapshots of simulations at ambient pressure (left) and pressures 68 GPa (middle) and 186 GPa (right). It is clearly seen that the share of the localized electrons in the interstitial space is greatly increased with pressure. In order to quantify the distribution of the localized share of the electron density we decomposed the electron density $\rho_{\rm el}(k,t)$ into two parts,

$$\rho_{\rm el}(k,t) = \rho_{\rm el}^{\rm scr}(k,t) + \rho_{\rm el}^{\rm orth}(k,t). \tag{11}$$

Here the first term on the right-hand side corresponds to the screening electron density that is spherically symmetrical around each ion and which follows the motion of ions, i.e., $\rho_{\rm ion}(k)$ due to Eq. (1). The second term on the right-hand side of Eq. (11) arises mainly from the nonspherical components of electron density distribution in the vicinity of ions. This part of the electron density is obtained as the orthogonalized one

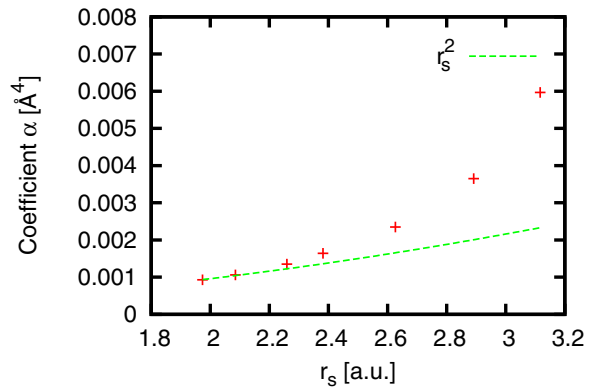

FIG. 7. (Color online) Dependence of the coefficent α at the long-wavelength limit of $S_{QQ}(k)$, Eq. (8), on the parameter r_s [28]. The quadratic dependence $\sim r_s^2$ predicted from RPA is valid at very high pressures and is shown with the dashed line.

to the ionic density:

$$\rho_{\rm el}^{\rm orth}(k,t) = \rho_{\rm el}(k,t) - \frac{\langle \rho_{\rm ion}(k)\rho_{\rm el}(-k)\rangle}{\langle \rho_{\rm ion}(k)\rho_{\rm ion}(-k)\rangle}\rho_{\rm ion}(k,t). \tag{12}$$

Then it is obvious that

$$\left\langle \rho_{\rm ion}(k)\rho_{\rm el}^{\rm orth}(-k)\right\rangle \equiv 0$$

and

$$\left\langle \rho_{\rm el}^{\rm scr}(k)\rho_{\rm el}^{\rm orth}(-k)\right\rangle \equiv 0,$$

which follow from Eq. (1).

In Fig. 9 we show the static correlator $S^{\rm orth}(k)$ at different pressures (left frame) and its peak positions compared to the locations of the $S_{QQ}(k)$. One can see that the share of the electron density, *which is mainly nonspherical around ions*, increases greatly with pressure, and the main peak of its structure factor $S^{\rm orth}(k)$ shifts to higher wave numbers with increasing pressure. It is obvious that the distance between the orthogonalized-to-ions parts of electron density should be larger than the distance between the ions. Therefore one can observe in the right frame of Fig. 9 that the main peaks in $S^{\rm orth}(k)$ at all studied pressures are located at smaller wave numbers as the corresponding main peaks of $S_{QQ}(k)$.

V. CHARGE-CHARGE AUTOCORRELATION FUNCTIONS IN LIQUID METALS

The linear response theory works perfectly in simple liquid metals. It allows us to estimate precisely the screening electron density (1) that follows the motion of ionic cores. Therefore $\rho_{\rm el}^{\rm scr}(r)$ can be used for the estimation of effective atom-atom potentials $V_{\rm eff}(r)$, which have been successfully used in molecular dynamics simulations of dynamic properties of liquid metals [6,32]. It is known, however, that in the case of liquid metals at high pressures and in covalent-bonded liquid metals the approach of effective pair atom-atom potentials is not working so good as in the simple liquid metals. It is obvious that the electron localization effects at extreme pressures [4,7] change the screening properties of the electron subsystem and cannot be precisely described by the linear response theory.

In Fig. 10 we show relaxation of the normalized density $F_{nn}(k,t)$ and total charge $F_{QQ}(k,t)$ autocorrelation functions in liquid Li at four different pressures. At small pressures the normalized autocorrelation functions are practically identical, while at pressures above 100 GPa we observed essential difference in the amplitude of the oscillations of both autocorrelation functions.

The time correlations of the total charge density are very interesting because, due to Eq. (11), there can be a deviation from the regular density autocorrelations

$$\frac{dQ(k,t)}{dt} = i\frac{1}{\sqrt{N}}Z_{\rm ion}\sum_i^N (\mathbf{k}\mathbf{v}_i)e^{-i\mathbf{k}\mathbf{R}_i(t)}$$
$$+\frac{d}{dt}\left[\rho_{\rm el}^{\rm scr}(k,t)+\rho_{\rm el}^{\rm orth}(k,t)\right] \equiv i\left(\mathbf{k}\mathbf{J}_{\rm tot}^{\rm scr}\right)+i\left(\mathbf{k}\mathbf{J}_{\rm el}^{\rm orth}\right),$$

where the $\mathbf{J}_{\rm tot}^{\rm scr}(k,t)$ is the screening current density composed of ions moving together with their screening electron cloud, and the $\mathbf{J}_{\rm el}^{\rm orth}(k,t)$ is the part of electron current density

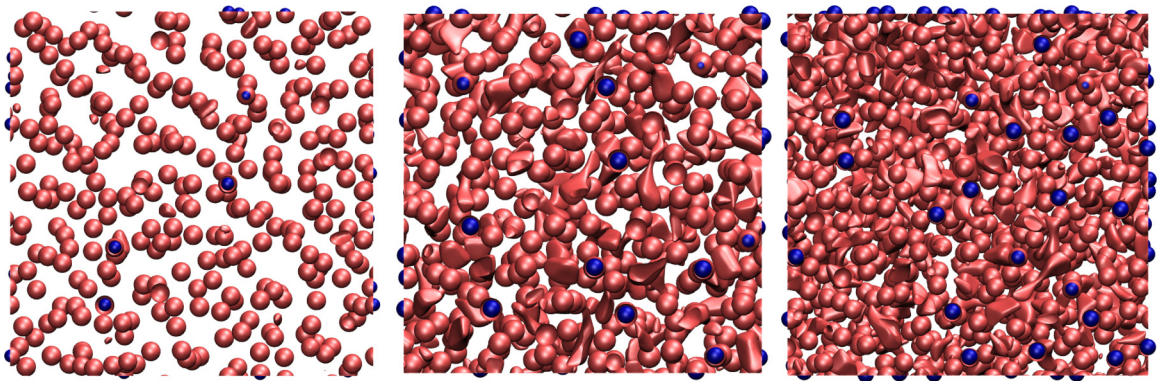

FIG. 8. (Color online) The isosurface (red shaded areas) of the ELF at the value 0.85 in snapshots of simulations at ambient pressure (left) and pressures 68 GPa (middle) and 186 GPa (right).

orthogonalized to the ionic positions. The latter can be connected to the localized part of electron density which according to the electron localization functions shown in Fig. 8 increases with pressure.

In order to get an insight into what kind of processes are responsible for different relaxation of $F_{QQ}(k,t)$ and $F_{nn}(k,t)$ we calculated the time correlation functions between the *orthogonalized-to-ions* part of the electron density. Having separated the part of the electron density orthogonalized to ionic positions we can confirm whether it takes part in an additional relaxation process at high pressure. For this purpose we calculated the corresponding time correlation function

$$F^{\mathrm{orth}}_{\mathrm{el-el}}(k,t) = \left\langle \rho^{\mathrm{orth}}_{\mathrm{el}}(k,t)\rho^{*,\mathrm{orth}}_{\mathrm{el}}(k,t=0)\right\rangle,$$

which in the case of liquid Li at pressure 186 GPa is shown in Fig. 11 at several wave numbers. A remarkable result is that in this time correlation function one observes the absence of the oscillations due to propagating collective excitations. The relaxation behavior of the $F^{\mathrm{orth}}_{\mathrm{el-el}}(k,t)$ implies that at high pressures there exists another relaxation process, which along with the standard thermal, structural, and shear relaxations [29,33] should be taken into account for generalized hydrodynamic description of the density correlations in liquid metals at high pressures. This relaxation process specific for high-pressure systems is defined by the part of the electron density which does not follow explicitly the motion of ions and can be represented by the nonspherical part of the distribution of the electron density around ions. It is obvious that since liquid Li at 1000 K remains metallic up to the highest pressures studied here, the strength of this relaxation of nonspherical parts should increase in the small-k region (as it is demonstrated in Fig. 11) and should follow the wave-number dependence according to Fig. 9.

VI. CONCLUSIONS

We have studied, using *ab initio* simulations, the behavior of charge correlations in a liquid metal in a wide range of pressures. Taking as a case study liquid Li, we studied the static and time-dependent quantities at pressures up to 186 GPa. We confirmed with the simulations of a large system of 600 particles the earlier found [3] tetrahedral clustering above 150 GPa.

We report here two main results:

(i) We predicted analytically, by making use of the linear response theory [9,10], that the total charge static structure factor $S_{QQ}(k)$ in metals has the long-wavelength asymptote $\sim k^4$. Our *ab initio* simulations of liquid Li at 1000 K and direct calculations of the $S_{QQ}(k) = \langle Q(k)Q(-k)\rangle$ showed perfect agreement with the theoretical long-wavelength asymptote. We point out that in ionic systems with localized electrons in the interstitial space the long-wavelength asymptote of $S_{QQ}(k)$ should be $\sim k^2$. Therefore the $S_{QQ}(k)$ can be a quantity that can be used to discriminate between a regular metal and pseudobinary compound, observed in potassium at high pressures [24].

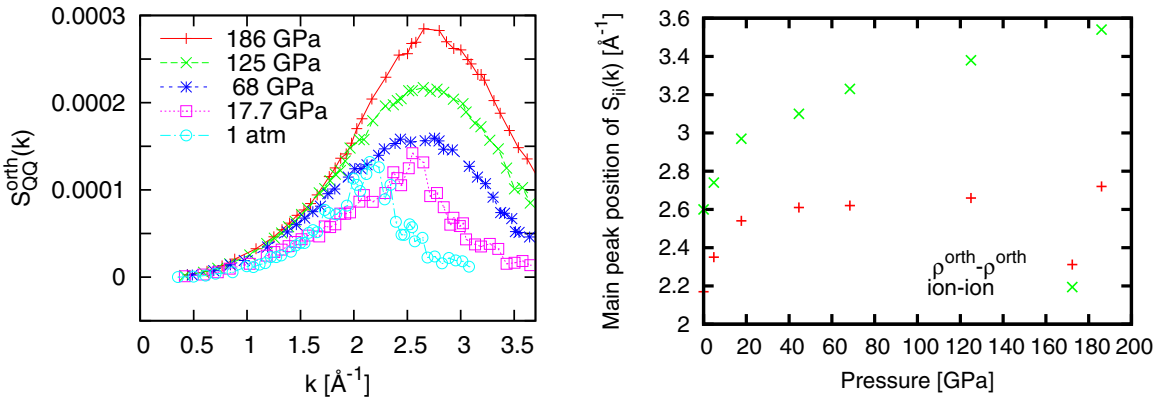

FIG. 9. (Color online) The static correlators of the electron density orthogonalized to the ionic positions (left panel), and the dependence of its peak location on the pressure together with the corresponding quantity from the ion-ion correlator (right panel).

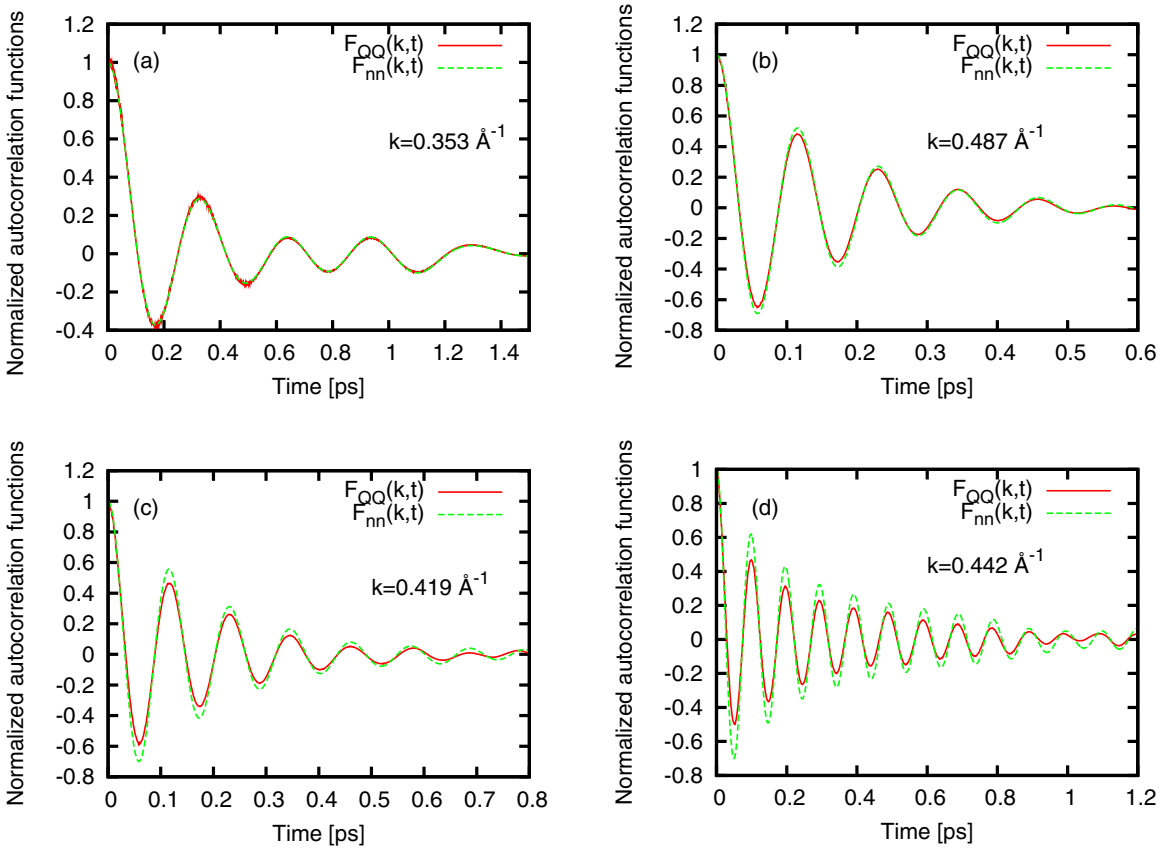

FIG. 10. (Color online) Total charge and density autocorrelation functions at ambient pressure (a), 68 GPa (b), 125 GPa (c), and 186 GPa (d).

(ii) We showed that in regular liquid metals at ambient pressure the linear response theory works perfectly well and due to almost perfect spherical screening the cloud of the electron density follows the motion of ions, resulting in the identical time-dependent behavior of the density-density and charge-charge correlations. This is why the pairwise, short-range effective potentials obtained from the linear response theory describe perfectly the dynamics of liquid alkali metals at ambient pressure. However the high pressure causes an essential increase of the nonspherical share of electron density around the ions and a part of electron density does not follow anymore the motion of ions. This is the reason why the approach of pair potentials does not work in metals at high pressures because of the increasing share of the nonspherical electron density distribution. We showed in the case of liquid Li that at high pressures the relaxation behavior of the density-demsity and charge-charge correlations is not anymore identical like it was at the ambient pressure. The deviation in this difference increased with the increase of the share of the nonspherical electron density distribution. We rationalized the role and behavior of the nonspherical share of electron density representing it via the contribution orthogonalized to ionic positions.

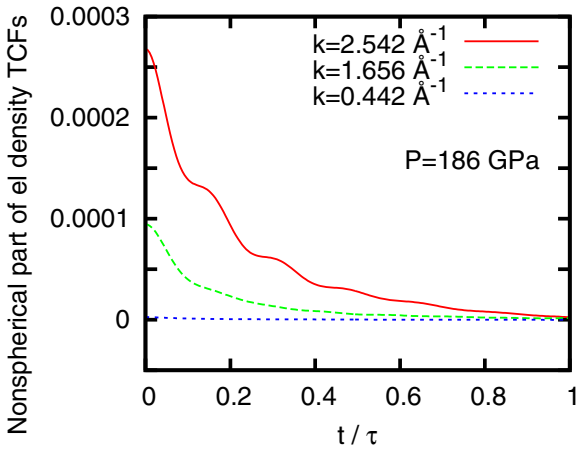

FIG. 11. (Color online) Relaxation of the autocorrelation between the part of the electron density orthogonalized to ionic positions. The time scale τ is equal to 0.20649 ps.

Remarkably the relaxation behavior of the orthogonalized part of the electron density to ionic positions can be another process that along with the thermal, structural, and shear relaxations should be taken into account in a generalized hydrodynamic description of liquid metals at high pressures.

ACKNOWLEDGMENT

The supercomputer allocation time in frames of the CINECA project "Dynamics and thermodynamics of compressed liquid metals studied by *ab initio* molecular dynamics" is gratefully acknowledged. The calculations have been performed using the *ab initio* total-energy and molecular dynamics program VASP (Vienna *ab initio* Simulation Program) developed at the Institut für Materialphysik of the Universität Wien [34–36].

[1] G. J. Ackland and I. R. Macleod, New J. Phys. **6**, 138 (2004).
[2] J.-Y. Raty, E. Schwegler, and S. A. Bonev, Nature (London) **449**, 448 (2007).
[3] I. Tamblyn, J.-Y. Raty, and S. A. Bonev, Phys. Rev. Lett. **101**, 075703 (2008).
[4] T. Bryk, S. De Panfilis, F. A. Gorelli, E. Gregoryanz, M. Krisch, G. Ruocco, M. Santoro, T. Scopigno, and A. P. Seitsonen, Phys. Rev. Lett. **111**, 077801 (2013).
[5] N. H. March, *Liquid Metals: Concepts and Theory* (Cambridge University Press, Cambridge, 1990).
[6] T. Scopigno, G. Ruocco, and F. Sette, Rev. Mod. Phys. **77**, 881 (2005).
[7] M. Marques, M. I. McMahon, E. Gregoryanz, M. Hanfland, C. L. Guillaume, C. J. Pickard, G. J. Ackland, and R. J. Nelmes, Phys. Rev. Lett. **106**, 095502 (2011).
[8] B. Rousseau and N. W. Ashcroft, Phys. Rev. Lett. **101**, 046407 (2008).
[9] J. Kohanoff and J.-P. Hansen, Phys. Rev. E **54**, 768 (1996).
[10] A. A. Louis and N. W. Ashcroft, Phys. Rev. Lett. **81**, 4456 (1998).
[11] E. Garcia Saiz, G. Gregori, D. O. Gericke, J. Vorberger, B. Barbrel, R. J. Clarke, R. R. Freeman, S. H. Glenzer, F. Y. Khattak, M. Koenig, O. L. Landen, D. Neely, P. Neumayer, M. M. Notley, A. Pelka, D. Price, M. Roth, M. Schollmeier, C. Spindloe, R. L. Weber, L. van Woerkom, K. Wünsch, and D. Riley, Nat. Phys. **4**, 940 (2008).
[12] M. P. Tosi, M. Parrinello, and N. H. March, Nuovo Cimento B **23**, 135 (1974).
[13] N. H. March, M. P. Tosi, and A. B. Bhatia, J. Phys. C: Solid State Phys. **6**, L59 (1973).
[14] J.-F. Wax, N. Jakse, and J.-L. Bretonnet, Phys. Rev. B **55**, 12099 (1997).
[15] M. Boulahbak, J.-F. Wax, N. Jakse, and J.-L. Bretonnet, J. Phys.: Condens. Matter **9**, 4017 (1997).
[16] S. K. Lai, K. Horii, and M. Iwamatsu, Phys. Rev. E **58**, 2227 (1998).
[17] J. Chihara and G. Kahl, Phys. Rev. B **58**, 5314 (1998).
[18] G. A. de Wijs, G. Pastore, A. Selloni, and W. van der Lugt, Phys. Rev. Lett. **75**, 4480 (1995).
[19] J. A. Anta, B. J. Jesson, and P. A. Madden, Phys. Rev. B **58**, 6124 (1998).
[20] T. Bryk and I. Klevets, J. Chem. Phys. **137**, 224508 (2012).
[21] T. Bryk and I. Klevets, Phys. Rev. B **87**, 104201 (2013).
[22] C. Massobrio and A. Pasquarello, Phys. Rev. B **68**, 020201(R) (2003).
[23] C. Massobrio, M. Celino, and A. Pasquarello, Phys. Rev. B **70**, 174202 (2004).
[24] M. Marques, G. J. Ackland, L. F. Lundegaard, G. Stinton, R. J. Nelmes, M. I. McMahon, and J. Contreras-Garcia, Phys. Rev. Lett. **103**, 115501 (2009).
[25] P. E. Blöchl, Phys. Rev. B **50**, 17953 (1994).
[26] G. Kresse and D. Joubert, Phys. Rev. B **59**, 1758 (1999).
[27] J. P. Perdew, K. Burke, and M. Ernzerhof, Phys. Rev. Lett. **77**, 3865 (1996).
[28] S. Ichimaru, Rev. Mod. Phys. **54**, 1017 (1982).
[29] J.-P. Hansen and I. R. McDonald, *Theory of Simple Liquids* (Academic, London, 1986).
[30] W. R. Magro, D. M. Ceperley, C. Pierleoni, and B. Bernu, Phys. Rev. Lett. **76**, 1240 (1996).
[31] A. D. Becke and K. E. Edgecombe, J. Chem. Phys. **92**, 5397 (1990).
[32] J. Hafner, *From Hamiltonians to Phase Diagrams: The Electronic and Statistical-Mechanical Theory of sp-Bonded Metals and Alloys*, Solid State Sciences Series, Vol. 70 (Springer, Berlin, 1987).
[33] J.-P. Boon and S. Yip, *Molecular Hydrodynamics* (McGraw-Hill, New York, 1980).
[34] G. Kresse and J. Hafner, Phys. Rev. B **47**, 558 (1993); **49**, 14251 (1994).
[35] G. Kresse and J. Furthmüller, Comput. Mater. Sci. **6**, 15 (1996).
[36] G. Kresse and J. Furthmüller, Phys. Rev. B **54**, 11169 (1996).